

Spectral Properties of Wall-Pressure Fluctuations and Their Estimation from Computational Fluid Dynamics

Daniel Juvé, Marion Berton and Edouard Salze

Abstract The various methods to obtain 1-point and 2-point statistical properties of wall-pressure fluctuations from CFD are described and discussed. If only averaged flow quantities are available through Reynolds Averaged Navier Stokes computations, empirical models or sophisticated statistical modeling have to be used to estimate wall-pressure spectra and spatial correlations. While very useful at design stage, their applicability to complex flows or geometries seems quite limited. Considering the rapid growth of computational power, it seems clear that the main pathway for the near future is to rely on time-dependent flow simulations, typically Large Eddy Simulations, and to estimate the pressure statistics through a posteriori signal processing. It seems also possible, at the moment only for relatively high Mach number flows, to estimate not only the hydrodynamic part but also the tiny acoustic contribution. Examples of computations of this acoustic contribution to wall-pressure are given together with related experiments.

1 Introduction

Estimating the statistical properties of the wall-pressure fluctuations induced by a turbulent flow is a necessary step to predict the vibroacoustic response of a structure. Typical examples are found in transportation systems, with a range of speeds varying from a few meters per second (for marine applications) to several hundred of meters per second (for aircraft applications). Classically, frequency spectra as

D. Juvé (✉) · M. Berton · E. Salze

Laboratoire de Mécanique des Fluides et d'Acoustique, UMR CNRS 5509, Ecole Centrale de Lyon, 36 Avenue Guy de Collongue, 69134 Ecully Cedex, France
e-mail: daniel.juve@ec-lyon.fr

M. Berton
e-mail: marion.berton@ec-lyon.fr

E. Salze
e-mail: edouard.salze@ec-lyon.fr

well as wave-number spectra are obtained using empirical models in which the global parameters of the flow enter and are evaluated using semi-analytical models (for example the boundary layer thickness is estimated using a simple flat plate formula). For the more complex geometries encountered in real configurations, it seems logical to rely on numerical simulations to obtain the required information. Today, Reynolds Averaged Navier Stokes (RANS) computations are performed routinely and are able to estimate accurately the global flow parameters at a reasonable computational cost. One important question is then: are the classical empirical models used to estimate the wall pressure statistical properties sufficient to predict for example the excitation of structures by flows under the influence of favorable or adverse pressure gradients or by detached flows induced by geometrical singularities of the surface?

To obtain more versatile models it seems desirable to rely more on numerical simulations at an earlier stage. Various approaches are possible depending on the nature of the numerical simulations. If only RANS simulations are available, a statistical model can be constructed in order to estimate the pressure spectra from the relatively poor information given by the RANS approach (typically a local value of the kinetic turbulent energy and of the dissipation rate). If unsteady computations are performed (such as Direct Numerical Simulations -DNS- or Large Eddy Simulations -LES-) a direct estimation of the time-evolution of the pressure fluctuations is possible from which statistical properties can be deduced by signal post-processing. Even with time-dependent simulations, a final and important difficulty persists if it is desirable to obtain not only the hydrodynamic contribution to wall-pressure but also the acoustic (compressible) contribution. In this case high fidelity compressible simulations are to be performed, and this is a particularly difficult task for low Mach number flows.

In aeroacoustics all these methods have been developed over the years and nearly routine unsteady computations are now performed to compute for example the noise generated by subsonic and supersonic aircraft propulsive jets [4, 5]. While the situation is clearly more difficult for wall bounded flows, such computations are already feasible for a number of applications or they will be feasible in a near future, due to the combination of rapidly growing available computational power and to the implementation of the high fidelity algorithms used in aeroacoustics.

In this paper we will give a short (and of course incomplete) review of the various approaches used to estimate wall pressure statistical properties with some illustration of today possibilities and shortcomings.

2 Fluid Dynamics and Wall-Pressure Fluctuations

To begin with, it may be useful to recall why the estimation of wall-pressure fluctuations is much more complicated than the determination of mean and turbulent velocity profiles.

The equations governing the flow are of course the Navier–Stokes equations. They are given by (we limit ourselves to incompressible flow for the moment):

$$\frac{\partial U_i}{\partial t} + U_j \frac{\partial U_i}{\partial x_j} = -\frac{1}{\rho} \frac{\partial p}{\partial x_i} + \nu \frac{\partial^2 U_i}{\partial x_i \partial x_j} \quad (1)$$

where U is the time-dependent local flow velocity, p the time-dependent local pressure, and ρ and ν the fluid density and kinematic viscosity.

It is natural to introduce the Reynolds decomposition of any time-dependent field as the sum of a mean part and a fluctuating part:

$$U_i = \bar{U}_i + u'_i; p = p_0 + p'$$

It is easily shown that the fluctuating pressure is then solution of a Poisson equation:

$$\frac{1}{\rho} \nabla^2 p' = -2 \frac{\partial \bar{U}_i}{\partial x_j} \frac{\partial u'_j}{\partial x_i} - \frac{\partial^2}{\partial x_i \partial x_j} (u'_i u'_j - \bar{u}'_i \bar{u}'_j) \quad (2)$$

The RHS of this equation can be considered as a forcing term involving the product of the gradient of the mean and of the fluctuating velocity and the double divergence of the centered product of velocity fluctuations; in other terms the sum of a linear contribution with respect to fluctuating quantities (or shear noise) and a non linear one (or self noise). Formally the solution of this equation can be written as the convolution product of the source term (ST) with an appropriate Green's function G :

$$p' = \rho G \times \text{ST} \quad (3)$$

In the presence of a flat plate (regarded as infinite), G is chosen as the half space Green's function

$$G = \frac{1}{2\pi} \frac{1}{|\mathbf{x} - \mathbf{y}|} \quad (4)$$

These formula emphasize the fact that the pressure at a given point depends on the whole velocity field around it, with a weighting function decreasing only slowly with the distance between the source and the receiver. In this sense the pressure can be considered as a non-local variable and it is the main reason why its statistical modeling is much more difficult than for velocity fluctuations.

To take into account compressibility effects (the acoustic part of the pressure fluctuations), the Poisson equation has to be replaced by the wave equation and the appropriate Green's function is simply the fundamental solution for the wave equation in half space (obtained for example by the method of images).

If a time-dependent fluid dynamics code can be used, the pressure fluctuations can be computed as a function of time using the Poisson equation in differential or integral form for incompressible flow. For compressible flow, one has to solve simultaneously the Navier-Stokes equations and an energy equation. Post-processing will give access (in principle at least) to all the needed statistical quantities. If only the Reynolds Averaged Navier-Stokes equations are solved a very difficult step of statistical modeling has to be performed. This is why today the large majority of the estimations of wall pressure statistical characteristics are based on empirical models, with RANS computations only used to determine the global flow properties.

3 Semi-empirical Models and RANS Computations

Let us have a look at the frequency-spectra first. The model which is considered as reproducing in the best way experimental data has been developed by Goody [13]. It is clearly an empirical model (as stated by Goody himself) even if it is based on earlier theoretical development by Chase and Howe; the overall form of the spectrum and its level have been adjusted to obtain the best possible fit with experimental data measured for a relatively large range of Reynolds number, but only for boundary layers without any external pressure gradient. Its form is as follows:

$$\frac{\Phi(\omega)}{\tau_w^2 \delta} = \frac{C_2(\omega\delta/U_e)^2}{\left[(\omega\delta/U_e)^{0.75} + C_1\right]^{3.7} + [C_3(\omega\delta/U_e)]^7} \quad (5)$$

In this formula, C_1 , C_2 and C_3 are 3 empirical constants; by fitting a large number of experimental data, Goody obtained $C_1 = 0.5$, $C_2 = 3$ while connecting C_3 to a sort of Reynolds number R_T

$$C_3 = 0.11R_T^{-0.57}; \quad R_T = R_\tau \frac{u_\tau}{U_e}$$

u_τ is the friction velocity and R_τ the Reynolds number based on this friction velocity and on the boundary layer thickness δ . U_e is the external flow velocity and τ_w the wall shear stress ($\tau_w = \rho u_\tau^2$).

The excellent agreement between Goody's formula and measured frequency spectra is illustrated on Fig. 1, where mixed variables have been used to normalize the spectra.

In the formula developed by Goody only global flow characteristics are used, and they can be easily obtained through a standard RANS computation. It is then tempting to use the same formula for flows (slightly) more complex than the TBL on a flat plate, but in view of the calibration process one can have some doubt about the validity of this approach.

One important case for practical applications is the development of a TBL in the presence of accelerating or decelerating flows induced by external pressure gradients

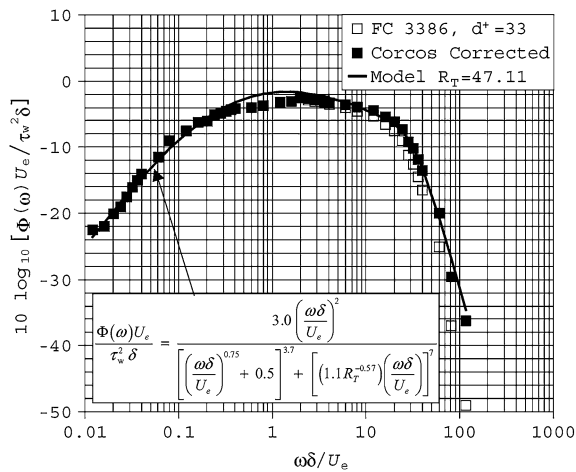


Fig. 1 Comparison of Goody’s model with the data of Farabee and Casarella; $Re_\theta = 3,386$. Figure reproduced from Ref. [13] with permission

or by curvature effects. Some years ago an experiment was conducted at ECLyon in order to study the influence of external pressure gradients created in a wind tunnel with an adjustable upper wall (ENABLE European program [23]). The geometry of the wind tunnel, placed in an anechoic environment, is shown in Fig. 2. To test Goody’s model in this configuration, we have run a RANS code (Ansys-Fluent $k - \omega$ or $k - \varepsilon$) and compared estimated spectra with the measured ones in different test sections to highlight the influence of the mean pressure gradient.

The comparisons were made for an inflow velocity equal to 50 m/s, the experimental spectra having been decontaminated from parasitic acoustic waves. A partial view of the computational mesh is shown in Fig. 3 together with computed velocity contours. A very fine mesh near the wall has been used in order to reproduce accurately the near wall region of the flow; the first point of the mesh in the direction normal to the lower wall was located at a distance of the order of 2–3

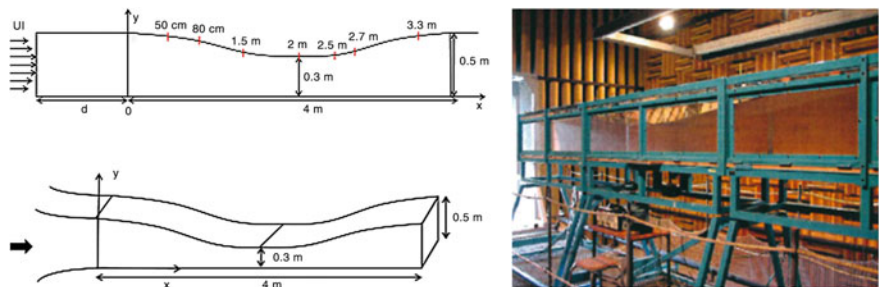


Fig. 2 Geometry and photograph of the wind tunnel with adjustable upper wall used in the ENABLE experiment

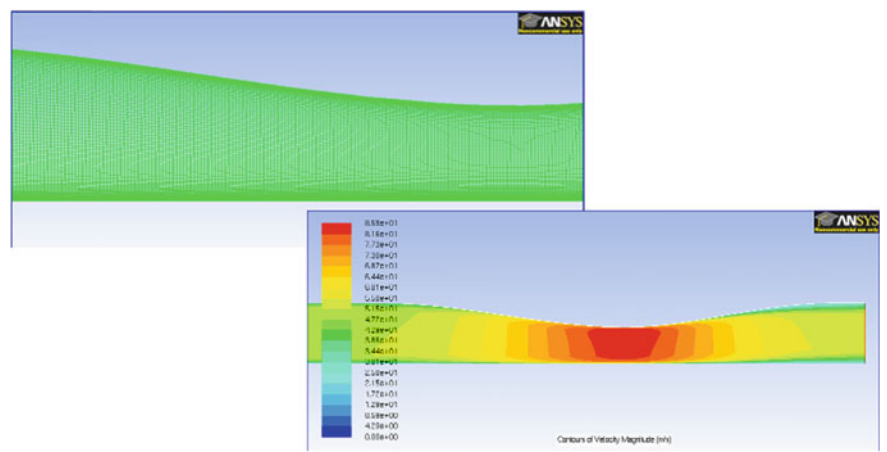
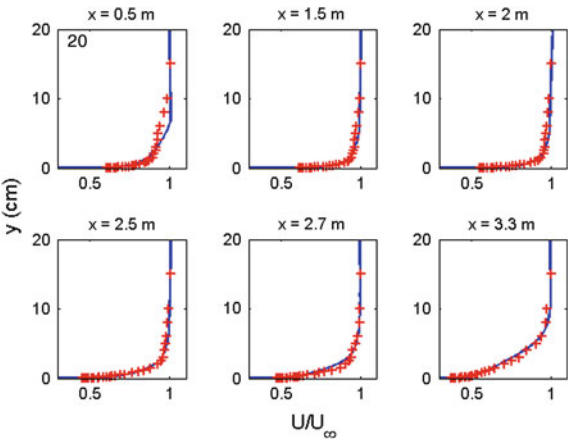


Fig. 3 Partial view of the numerical mesh and velocity contours computed in the RANS simulation of the ENABLE experiment

wall units only. A comparison of measured and calculated velocity profiles is given in Fig. 4 to demonstrate the very good agreement obtained; agreement with measured values of the wall shear-stress along the duct was also excellent.

Figure 5 displays the spectra measured and computed using Goody’s formula at $x = 0.5$ m, where the external pressure gradient is very nearly zero (ZPG case). It can be shown that Goody’s model does a very good job, reproducing both overall shape and level (within 1–2 dB). But in the diverging part of the wind tunnel (decelerating flow, Adverse Pressure Gradient), things are radically different (Fig. 6). The estimated spectrum is quite far from the experimental one and it underestimates the low-medium part of the spectrum by up to 12 dB!. It is also to be noted that the predicted general shape is also completely at variance with the

Fig. 4 Comparison between measured and computed velocity profiles along the ENABLE wind tunnel



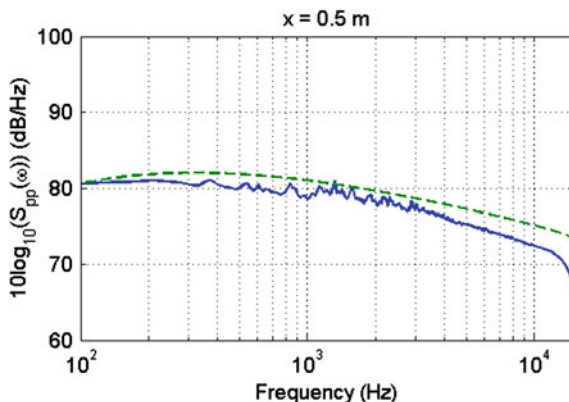


Fig. 5 Comparison between measured and estimated wall pressure spectrum using Goody's model and RANS flow computation for the ENABLE experiment; Zero Pressure Gradient case (in *continuous blue line* experimental data; in *green dashed line* Goody's model)

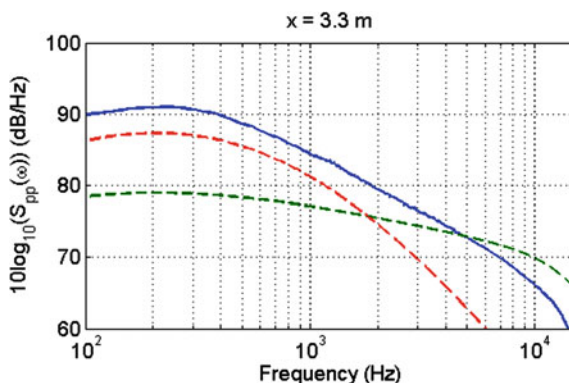


Fig. 6 Comparison between measured and estimated wall pressure spectrum using Goody's model and RANS flow computation for the ENABLE experiment; Adverse Pressure Gradient case (in *continuous blue line* experimental data; in *green dashed line* Goody's model; in *red dashed line* Rozenberg's model)

measured one. This lack of validity of Goody's formula in APG conditions has been already noted by other researchers and recently Rozenberg et al. [24] have proposed a modification of the initial model to deal with APG encountered on airfoils near the trailing edge. The result of Rozenberg's model is also shown on Fig. 6, and it is clear that it does a far better job than the classical one even if significant differences are noted at high frequency. Unfortunately the empirical character of the new model is even more pronounced than the model by Goody and its applicability in situations with different values of the pressure gradient is questionable. When trying to use it in the first part of the wind tunnel where the flow is accelerated (Favorable Pressure Gradient) we obtained very bad results; in fact the quality of the estimation

was worse than with Goody's model. In Fig. 7 we have plotted only the comparison of Goody's formula with experimental data; in this case the model overestimates the measured spectrum level by 5 dB typically.

The main conclusion at this stage is that empirical models do a good job when applied to classical configurations (for which they have been calibrated!) but are unable to be predictive in slightly different situations as exemplified for TBL with external pressure gradients, a case encountered in most practical applications in transportation systems. It seems clear that this difficulty of using empirical models for frequency spectra will be increased when 2-point statistical quantities, such as space-time cross-correlations of wave-number spectra, have to be estimated for computing flow induced vibration and noise.

Certainly the most used formula for evaluating the 2D wave-number spectrum of pressure fluctuations is the Chase model [6, 7]. This model is highly empirical and involves up to 7 adjustable coefficients when extrapolated to cover both the hydrodynamic region and the acoustic domain (plus another parameter controlling the level of the spectral peak at $k = k_0$, see for example Howe [16]). We give below the form limited to the hydrodynamic domain, depending on 4 adjustable coefficients.

$$\frac{\Phi(k, \omega)}{\rho^2 u_\tau^3 \delta^3} = \frac{1}{[(k_+ \delta)^2 + 1/b^2]^{5/2}} \left[C_M (k_1 \delta)^2 + C_T (k \delta)^2 \frac{(k_+ \delta)^2 + 1/b^2}{(k \delta)^2 + 1/b^2} \right] \quad (6)$$

$$k_+^2 = (\omega - U_c k_1)^2 / (h u_\tau)^2 + k^2$$

$$M = U/c_0 \ll 1; \quad k \gg \omega/c_0; \quad \omega \delta/U > 1$$

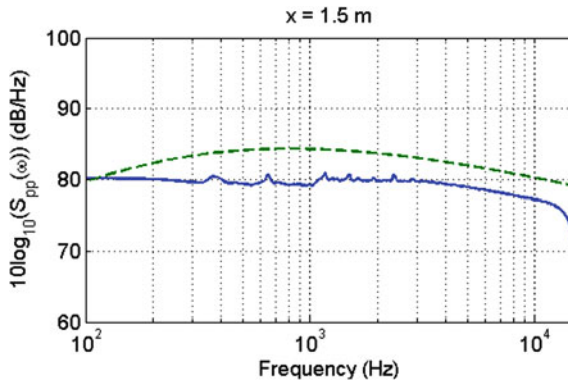


Fig. 7 Comparison between measured and estimated wall pressure spectrum using Goody's model and RANS flow computation for the ENABLE experiment; Favorable Pressure Gradient case (in continuous blue line experimental data; in green dashed line Goody's model)

The adjustable coefficients have been fixed by comparison with experiment and the recommended values are

$$b \approx 0.75; \quad C_M \approx 0.1553; \quad C_T \approx 0.0047; \quad h \approx 3$$

C_M and C_T correspond to the contributions to wall pressure fluctuations of the shear and self terms respectively.

Experiments in which wave-number spectra have been measured are very rare, so that this formula (and other empirical ones) can be considered as reliable only near the convective ridge; there are some doubts about its validity in the subconvective region, and the situation is even worse in the acoustic domain where the validity of the complete formula has not been confirmed by experiment. Moreover it is doubtful that such models can be applied in the presence of external pressure gradients, curvature effects or rough surfaces. It is then clearly desirable to develop a less empirical approach relying on more detailed flow computations.

3.1 Statistical Modeling

In aeroacoustics, the purely empirical approach has been progressively abandoned and methods based on a statistical modeling of jet noise are now used routinely for example with the MGB code or some other code based on the work by Tam and Auriault [28] for example. For wall-pressure fluctuations the only paper dealing with this approach is due to Peltier and Hambric [22]. There are good reasons for the very limited amount of work done along that line. Compared to jet free flows, wall-bounded flows are much more complicated to model; they are highly non homogeneous and anisotropic and the range of involved turbulent eddies is very large. Another reason is the close vicinity between sources and observation point; it is then not possible to use any asymptotic expansion of the Green's function (a near-field situation as opposed to a far-field situation, common in aeroacoustics applications).

To compute wall-pressure spectra it is necessary to estimate correlation functions or their equivalent in Fourier space (wave-number spectra). Starting with the equation for the fluctuating pressure (Eq. 2), it is possible to build a formula for space-time correlation functions; in a very symbolic form (and assuming dependence only on space and time separations) it can be written as:

$$R_{p'p'}(\Delta \mathbf{x}_s, \tau) \propto \int \int \left(U_i U_j R_{u'_k u'_l} + R_{u'_l u'_k} \right) dy dy' \quad (7)$$

with $\mathbf{x}_s = (x_1, x_2)$ denoting coordinates in the wall plane (x_1 is aligned with the mean flow).

The wave-number frequency spectrum is then obtained by a Fourier transform with regard to space and time:

$$\Phi_{p'p'}(\mathbf{k}, \omega) = FT_{\Delta \mathbf{x}_s, \tau} [R_{p'p'}(\Delta \mathbf{x}_s, \tau)] \quad (8)$$

with $\mathbf{k} = (k_1, k_2)$ the conjugate coordinate of \mathbf{x}_s in the wall plane.

This formula involves the double volume integration of two spatial correlation functions of velocity fluctuations; one is a second order correlation tensor (involving gradients of the mean flow velocity, a Mean Flow-Turbulence interaction or shear-noise term) and the second one is a fourth order correlation tensor (Turbulence-Turbulence interaction term or self-noise). It should be kept in mind that the available information given by RANS computations for the turbulent fluctuations is very limited. Usually only the local values of the turbulent kinetic energy k and of the dissipation rate ε are available ($k - \varepsilon$ model). It is then necessary to perform a large modeling effort to link the needed cross-correlations to these values. Typically one has to reduce 2-point correlations to 1-point information by assuming a given shape of the space and time correlations (a Gaussian shape in general) and to estimate the time and length scales defining the decay rate of these correlations by using dimensional arguments:

$$L \propto \frac{\varepsilon}{k^{3/2}}; \quad T \propto \frac{\varepsilon}{k^2} \quad (9)$$

The proportionality coefficients are obtained by fitting experimental data obtained in TBL flows. In fact the situation is quite complex as the turbulence is highly non homogeneous and non isotropic. The modeling has to be accurate for a very large range of turbulent scales in terms of non dimensional wall units $y^+ = yu_\tau/\nu$ (y is here the distance normal to the surface). Let us take a simple numerical example for a TBL in air with an external velocity of and a plate of length 1 m; this gives a boundary thickness of the order of 2 cm and a viscous length scale of only 10 μm ; as the peak of turbulent intensity occurs for $y^+ \approx 20$ (see the review paper by Smits et al. [27]), the modeling has to cover correctly a range of several hundred of wall units. Details of the modeling approach will be found in the paper by Peltier and Hambric [22] in which point frequency spectra are computed and compared to Schloemer's data for APG and FPG as well as ZPG conditions. The authors obtained good agreement with Schloemer's data [26] after tuning their model, and the influence of APG and FPG is relatively well captured (Fig. 8).

In principle the approach developed by Peltier and Hambric is able to estimate not only point frequency spectra but also space-time correlations of wall pressure fluctuations, but no attempt has been done in the cited paper nor in other work, to the best of our knowledge.

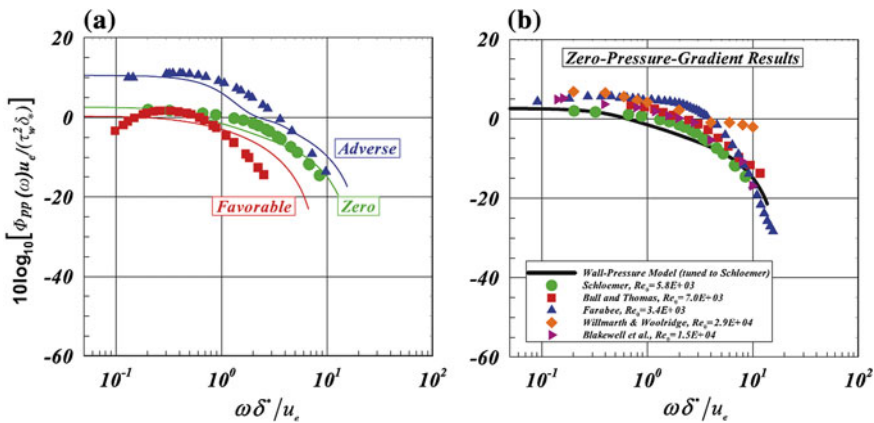


Fig. 8 Predicted wall-pressure spectra using statistical modeling compared to **a** Schloemer's data for favorable, zero and adverse pressure gradients, and **b** to data of several authors for zero pressure gradient conditions. Figure reproduced from Peltier and Hambric [22] with permission

4 Time-Resolved Incompressible CFD and Wall-Pressure Fluctuations

Due to the intrinsic limitations of empirical models and even of statistical modeling based on RANS computations, a number of authors have tried to estimate wall pressure fluctuations directly from time-dependent numerical simulations. One of the main difficulties is the range of turbulent scales to be computed and for this reason most of the published results do not consider true boundary layers, but fully developed channel flows; they are less demanding in terms of computational power as periodic boundary conditions and spectral methods in the 3 directions can be used (at least for incompressible flow).

4.1 Direct Numerical and Large Eddy Simulations

When speaking of time-dependent Navier-Stokes computations, two main possibilities exist, the Direct Numerical Simulation (DNS) and the Large Eddy Simulation (LES). In DNS the numerical mesh has to resolve all the turbulent scales from the largest ones to the ultimate Kolmogorov scale, where viscosity effects become dominant. In LES, only the most energetic scales are resolved and the influence of the smaller scales (or subgrid scales) is modeled via typically a turbulent viscosity approach. DNS is exact as no modeling of turbulence is needed, but extremely demanding in terms of computational power and thus limited to relatively low Reynolds number flows, whereas LES is less demanding and thus can be applied (with care!) to more realistic flows. The numerical cost is however important even

in LES as in the direction normal to the wall it is necessary to use a very refined mesh in order to capture the most energetic region, located very close to the wall for moderate to high values of the Reynolds number.

A final, and important, point is the choice between incompressible or compressible computations. Most of the published papers are dealing with incompressible flow, which is very reasonable from the purely fluid mechanics point of view, the Mach number being in general quite low. But we, acousticians, know that in a number of practical cases it is necessary to estimate also the acoustic contribution to the wave-number spectrum. This is clearly needed if the sound generated by the TBL has to be computed (aerodynamic noise in the sense of Lighthill), but this is also often the case to determine flow induced vibrations and the noise generated by these vibrations. An instructive discussion and numerical examples can be found for example in the excellent papers by Graham [14, 15]. Computing the tiny acoustic contribution (as compared to the incompressible or hydrodynamic contribution) is a very difficult challenge. Great progress has been made in recent years in aeroacoustics in the computation of the noise generated by jets and airfoils, but the application to TBL has only been attempted very recently.

4.2 Progress in Numerical Estimation of Wall Pressure Fluctuations

The first estimations of the statistical properties of wall pressure fluctuations date back to the end of the 80s (Kim [19], Choi and Moin [8]). The data base used by Choi and Moin was obtained from a DNS of a channel flow, for a small value of the Reynolds number based on the center-line velocity and on the channel half height ($Re_h = 3,200$) or for the more relevant Reynolds number based on the boundary layer momentum thickness, $Re_\theta = 287$; these values are typically 10–100 times lower than those measured in classical experiments. Point-spectra, correlations and wave-number spectra were displayed and compared to experimental data. The number of grid points was of the order of 2 millions and the resolution of frequency spectra was typically limited to values of the reduced frequency $\omega\theta/U_e$ of order unity. The main problem with DNS is that the relation between the Reynolds number and the number of required grid points is $N \propto Re^{9/4}$. So multiplying the Reynolds number by a factor of 10 requires multiplying the number of grid points by nearly 200!

In the following years the range of simulated frequencies has only slowly evolved, in direct relation with the increase of available computational power. Na and Moin [21] in 1998 for example studied a separated boundary layer, using 13 million grid points, and more recently (in 2006), Hu et al. [17] performed a huge computation of a channel flow with 520 million grid points. They were able to simulate channel flow up to $Re_\tau = 1,400$ (Reynolds number based on the friction velocity), a value comparable to the experimental ones. One of their typical result is

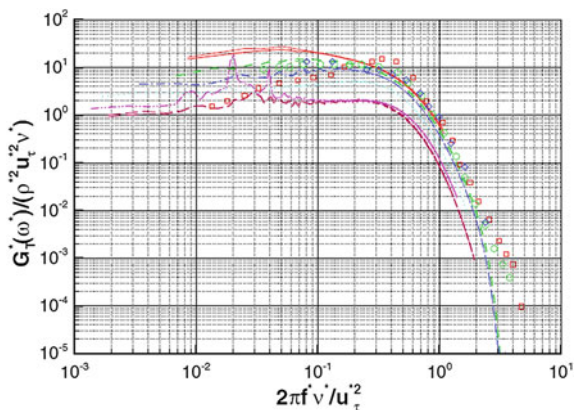


Fig. 9 Point spectrum of wall pressure fluctuations evaluated from a DNS computation and compared with experiments. Channel flow simulation for $Re_\tau = 720$, $Re_\theta = 1,343$. Figure reproduced from Hu et al. [17] with permission

displayed in Fig. 9. The comparison of spectra shows a good agreement for the overall shape, but the numerical simulations seem to underestimate the levels (for comparable values of the Reynolds number). It is very surprising, and quite unfortunate considering the huge data base available, that the authors do not mention any 2-point results, such as wave-number frequency spectra.

At this stage two important points need attention: is it possible to simulate a true boundary layer flow at a reasonably high value of the Reynolds number? And, is it possible to do that with compressibility taken into account, in order to estimate the acoustic contribution to wall pressure statistics?

5 The Acoustic Contribution to Wall-Pressure Fluctuations

The estimation of the full wave-number spectrum is a formidable task both from the experimental point of view and from the numerical one. The number of experiments in which at least a 1-D spectrum is available is quite limited, not to speak of 2-D spectra.

5.1 Experimental Results

Obtaining the wave-number spectrum can be done directly (using 2D arrays of sensors) or indirectly by computing first cross-correlations and then taking a spatial Fourier transform. The first approach is nearly out of reach due to the very large number of sensors needed to cover both high spatial frequencies (hydrodynamic

contribution) and low spatial frequencies (acoustic contribution). 1D spectra can be obtained using a linear array of sensors (aligned with the mean flow) but it should be kept in mind that 1D spectra integrate the contributions of all wave-vectors projected along the array direction. Example of direct measurement of the 1D streamwise spectra can be found in the paper by Abraham and Keith [1] who used a linear array of 48 microphones. The quality of the measurements far from the convective ridge was limited by aliasing and array side lobes; comparison with the Corcos [9] and Chase [7] models was nevertheless possible, and a relatively good agreement with the latter was obtained in the subconvective region. The acoustic region was not specifically studied in this paper.

Recently an experiment was developed at ECLyon (in collaboration with Renault) in order to estimate the 2D wave-number spectrum both in the convective region and in the acoustic domain. For automotive applications it is indeed thought that the (very small) acoustic contribution to the wall pressure field can nevertheless contribute significantly to vehicle interior noise as it is considerably less filtered out by the windshield than the hydrodynamic contribution in a certain range of audible frequencies. The experimental details and the main results are to be found in a PhD Thesis [2] and in a JASA paper [3].

A linear array of 63 microphones was mounted on a rotating disk (see Fig. 10), and the cross-spectra were measured for 63 angular positions; the flow speed was varied from 33 to 54 m/s. The wave-number frequency spectrum was then obtained through a 2D discrete spatial Fourier transform for a useful range of frequencies extending approximately from 500 Hz to 5 kHz. One of the main results of the study by Arguillat [2] concerns the ratio of the acoustic Power Spectral Density (PSD) to the hydrodynamic PSD; it was found to be of the order of 3 % (−15 dB) with very little variations with frequency (Fig. 11). This value seems a bit high (but we just do not have any reference value available, theoretically or experimentally), may be due to confinement in the wind tunnel cross-section.

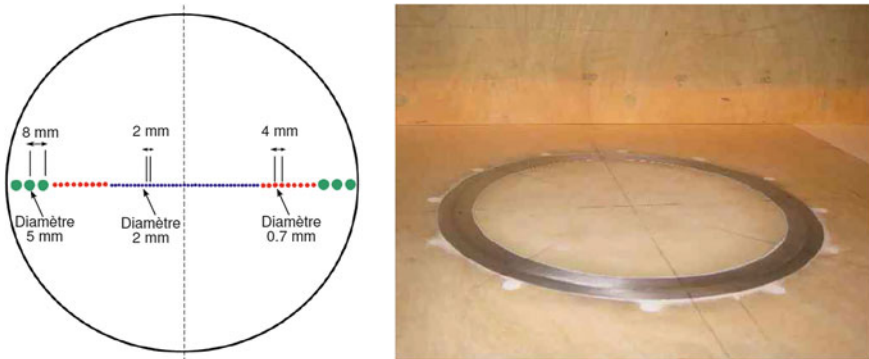


Fig. 10 Arrangement of the linear array used in the Arguillat experiment [2] and of the rotating disk inserted in the lower wall of the wind tunnel

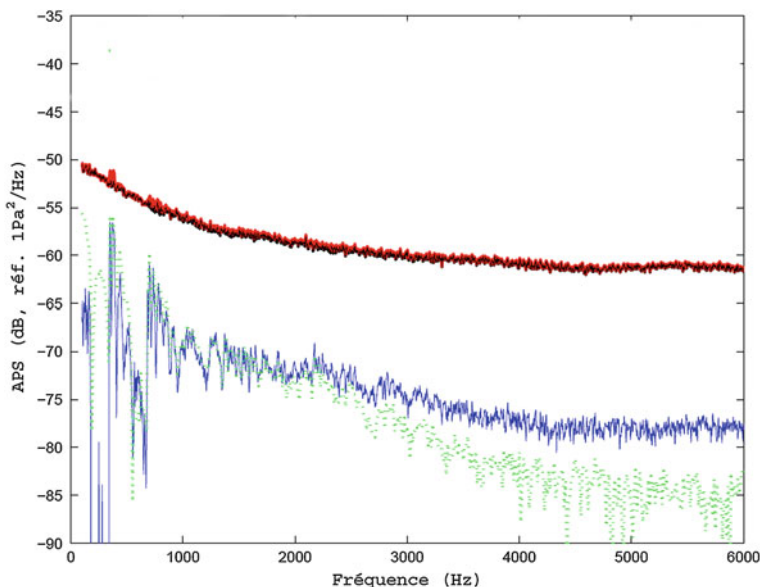


Fig. 11 Estimation of the relative contribution of the acoustic and hydrodynamic regions to the wall pressure spectrum in the experiment by Arguillat. The full spectrum and the hydrodynamic contribution are nearly undiscernable (*upper curves*) and the acoustic contribution is some 15 dB lower whatever the frequency; the acoustic contribution has been evaluated by integration of the 2D wave-number spectrum over the radiation disk (*blue line*) and by fitting a Corcos-like model to the data (*green line*)

To verify this, and to extend the range of applications, a new experimental set-up was designed at ECLyon. The objectives were first to enhance signal processing relative to the Arguillat experiment; a larger disk was used and a different arrangement of the microphones along the array was chosen in order to increase the array resolution and to reduce side lobes; potential contamination by parasitic acoustic noise was reduced by installing acoustic liners inside parts of the wind tunnel. The second goal was to study the influence of external pressure gradients (APG and FPG) generated by tilting part of the upper wall, and this up to a maximum velocity of around 100 m/s (details can be found in [25]). In parallel numerical simulations are performed by X. Gloerfelt using high fidelity compressible LES (ANR SONOBL program). The experiments are on their way, but preliminary results are very encouraging; as an example we show on Fig. 12 two k_1 – k_2 wave-number spectra obtained for an external velocity of 45 m/s at 500 and 1,000 Hz respectively. The color maps are much cleaner than in the Arguillat experiment, with the influence of side lobes being considerably reduced; as a result the acoustic disk as well as the convective region are clearly visible.

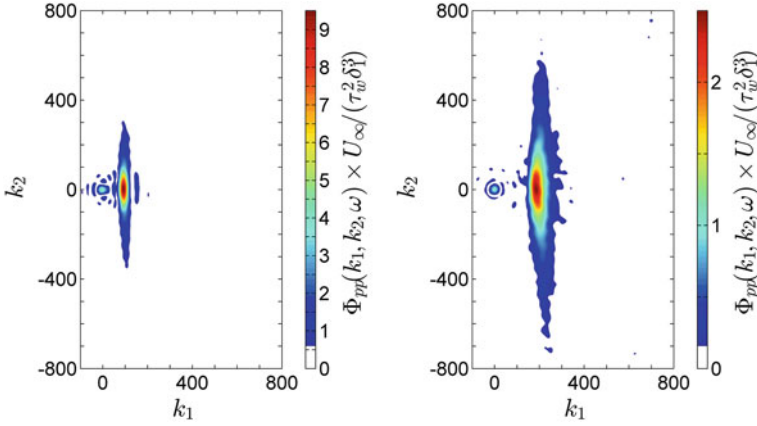


Fig. 12 Normalised 2D wave-number spectra of wall pressure fluctuations measured in the SONOBL experiment for two frequencies, $f = 500$ Hz (*left*) and $f = 1,000$ Hz (*right*). Incoming velocity $U_e = 45$ m/s; Zero Pressure Gradient case. More details will be found in [25]

5.2 Numerical Simulations

Numerical simulations mimicking the SONOBL experiment are still in progress. However Gloerfelt and Berland [12] have very recently published results for a spatially developing TBL for a higher value of the Mach number (0.5 instead of 0.1–0.3 in our experiments). They used high order, high precision algorithms to solve the 3D fully compressible Navier-Stokes equations, and were able to compute both the noise radiated outside the boundary layer and the wall pressure fluctuations. Three figures will illustrate this very original and interesting work.

Figure 13 displays a point frequency spectrum scaled by inner variables, and compared to experimental data and to Goody's model. Up to the frequency cut-off of the LES (imposed by the numerical grid, with 54 millions of points) the computed spectrum agrees very well with the data, in shape and level. Figure 14 displays a cut at $k_2 = 0$ of 2D wave-number spectra (not to be confused with the spanwise spectrum measured by 1D arrays) obtained for various values of the reduced frequency $\omega\theta/U_e$. The evolution with the frequency of the convective ridge is very apparent with a maximum around $k_1 = \omega/U_c$ ($U_c = 0.8U_e$ is the convection velocity), but, much more important, a peak associated to acoustic disturbances is clearly seen around $k_1 = \omega/c_{\text{eff}}$, especially for the two higher frequencies (c_{eff} is an effective sound speed accounting for the convection of acoustic waves by the rapid mean flow). And finally we display a color map of $\Phi_{pp}(k_1, k_2 = 0, \omega)$ on Fig. 15.

The hydrodynamic part is clearly seen with its well-known non symmetric pattern toward the subconvective or superconvective regions, but much more

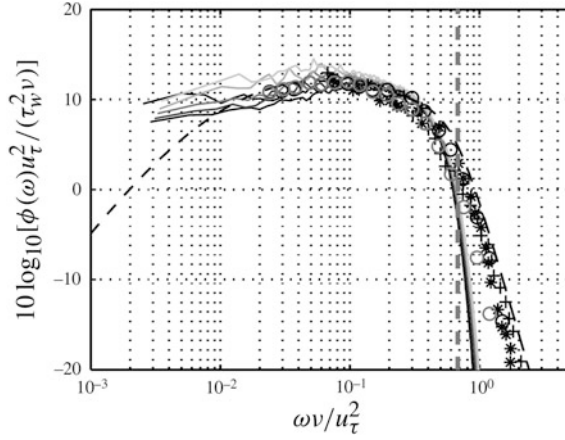


Fig. 13 Frequency power spectra of wall pressure fluctuations computed from a LES of a spatially developing TBL (*solid line*) and compared to various experimental data sets (*symbols*) and to Goody's model (*dashed line*). The *vertical dashed line* indicates the frequency cut-off of the LES. Figure reproduced from Gloerfelt and Berland [12] with permission

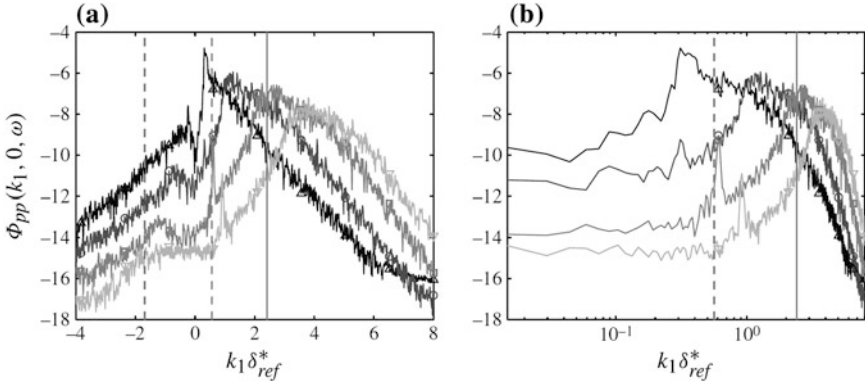


Fig. 14 Wavenumber-frequency spectra computed from LES for different non-dimensional frequencies (δ^* denotes the boundary layer displacement thickness). The *solid vertical line* indicates the convective wavenumber and the *vertical dashed line* the convected acoustic wavenumber; they are associated with the curve corresponding to the third highest frequency, for which a very distinct peak is seen near the acoustic wavenumber. Figure reproduced from Gloerfelt and Berland [12] with permission

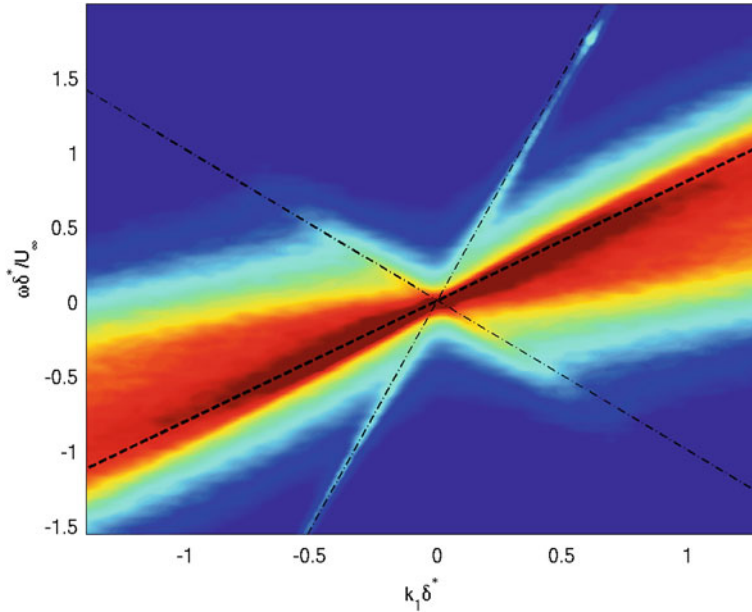


Fig. 15 Color map of the wavenumber-frequency spectrum (dB scale) computed from LES for a large range of non-dimensional frequencies. The *thick dashed line* represents the convection of turbulent structures ($k_c = \omega / U_c$; $U_c = 0.6 U_e$) and the *light dashed lines* correspond to acoustic waves convected by the mean flow ($k_+ = \omega / (U_e + c_0)$ and $k_- = \omega / (U_e - c_0)$). Figure courtesy of X. Gloerfelt

important are the characteristic lines showing the acoustic contribution convected upstream and downstream with effective velocities equal to $c_0 - U_e$ and $c_0 + U_e$ respectively.

6 Conclusion

In this paper we have given a rapid description of the various methods used to estimate the statistical properties of wall pressure fluctuations from CFD data: empirical models fed by RANS global flow characteristics, statistical modeling relying on local values of turbulent intensity and turbulent space and time scales, and finally time-dependent Navier-Stokes simulations (DNS or LES).

Empirical models are clearly useful at a first design stage, but their applicability is limited to the cases where they have been calibrated, i.e. typically turbulent boundary layers over flat surfaces; even the relatively simple extension of TBL in the presence of an external pressure gradient necessitates non trivial adjustments of the models for point frequency spectra. The statistical modeling of Peltier and Hambric [22] is attractive but, up to now, it has been developed only for the

estimation of point spectra, not for 2-point correlations. One possible extension would be to use LES instead of RANS computations to inform the statistical model, an approach recently put forward for jet noise computation [18].

It seems however that the time-dependent computation of pressure fluctuations by solving the Navier-Stokes equations is the main pathway for the (near) future. Considering the range of Reynolds numbers encountered in the applications, LES is certainly to be preferred to DNS, at the expense of not being able to compute the influence of the smaller turbulent scales (introducing a high frequency cut-off). For applications in which the Mach number is not too small, a compressible computation will even be possible to determine the acoustic contribution to wall pressure fluctuations (this is already possible for high Mach number flows). In this context it should be noted that an alternative computational method, the Lattice Boltzmann Method, has shown also a great potential. Of course new experimental data, more precise and in well-controlled conditions, are needed to validate the computations (but it should be kept in mind that in some cases numerical simulations can be more appropriate than experiments!). Very recently a number of teams have been working in this direction, developing new facilities and new measurement techniques [10, 11, 20]. It can thus be expected that this combined effort in the numerical and experimental directions will shed some new light in a near future on this old and difficult problem.

Acknowledgments The authors have benefited from fruitful discussions with and inputs by Christophe Bailly, Xavier Gloerfelt and Gilles Robert. This work was performed within the framework of the Labex CeLyA of Université de Lyon, operated by the French National Research Agency (ANR-10-LABX-0060/ANR-11-IDEX-0007). Financial support of Marion Berton by DCNS Research is also acknowledged.

References

1. B.M. Abraham, W.L. Keith, Direct measurements of turbulent boundary layer wall pressure wavenumber-frequency spectra. *J. Fluid Eng.* **120**, 29–39 (1998)
2. B. Arguillat, Etude expérimentale et numérique de champs de pression pariétale dans l'espace des nombres d'onde, avec application aux vitrages automobiles, Ph.D. thesis, Ecole centrale de Lyon, 2006, pp. 2006–2014
3. B. Arguillat, D. Ricot, C. Bailly, G. Robert, Measured wavenumber-frequency spectrum associated with acoustic and aerodynamic wall pressure fluctuations. *J. Acoust. Soc. Am.* **128** (4), 1647–1655 (2010)
4. C. Bailly, C. Bogey, O. Marsden, Progress in direct noise computation. *Int. J. Aeroacoustics* **9** (1–2), 123–143 (2011)
5. C. Bogey, O. Marsden, C. Bailly, Influence of initial turbulence level on the flow and sound fields of a subsonic jet at a diameter-based Reynolds number of 10^5 . *J. Fluid Mech.* **701**, 352–385 (2012)
6. D.M. Chase, Modeling the wavevector-frequency spectrum of turbulent boundary layer wall pressure. *J. Sound Vib.* **70**(1), 29–67 (1980)
7. D.M. Chase, The character of turbulent wall pressure spectrum at subconvective wavenumbers and a suggested comprehensive model. *J. Sound Vib.* **112**, 125–147 (1987)

8. H. Choi, P. Moin, On the space-time characteristics of wall pressure fluctuations. *Phys. Fluids A* **2**, 1450–1460 (1990)
9. G.M. Corcos, The structure of turbulent pressure field in boundary layer flows. *J. Fluid Mech.* **18**(3), 353–378 (1964)
10. K. Ehrenfried, L. Koop, Experimental study of pressure fluctuations beneath a compressible turbulent boundary layer. In: 14th AIAA/CEAS Aeroacoustics Conference, AIAA Paper (2008), pp. 2008–2800
11. C. Gabriel, S. Müller, F. Ullrich, R. Lerch, A new kind of sensor array for measuring spatial coherence of surface pressure on a car's side window. *J. Sound Vib.* **333**, 901–915 (2014)
12. X. Gloerfelt, J. Berland, Turbulent boundary layer noise: direct radiation at Mach number 0.5. *J. Fluid Mech.* **723**, 318–351 (2013)
13. M. Goody, Empirical spectral model of surface pressure fluctuations. *AIAA J.* **42**(9), 1788–1794 (2004)
14. W.R. Graham, Boundary layer induced noise in aircraft, part I: the flat plate model. *J. Sound Vib.* **192**(1), 101–120 (1996)
15. W.R. Graham, A comparison of models for the wavenumber-frequency spectrum of turbulent boundary layer pressures. *J. Sound Vib.* **206**(4), 541–565 (1997)
16. M.S. Howe, *Acoustics of Fluid Structure Interactions* (Cambridge University Press, Cambridge, 1998)
17. Z.W. Hu, C.L. Morfey, N.D. Sandham, Wall pressure and shear stress spectra from direct simulations of channel flow. *AIAA J.* **44**(7), 1541–1549 (2006)
18. S.A. Karabasov, M.Z. Afsar, T.P. Hynes, A.P. Dowling, W.A. McMullan, C.D. Pokora, G.J. Page, J.J. McGuirk, Jet noise: acoustic analogy informed by large eddy simulation. *AIAA J.* **48**(7), 1312–1325 (2010)
19. J. Kim, On the structure of pressure fluctuations in simulated turbulent channel flow. *J. Fluid Mech.* **205**, 421–451 (1989)
20. D. Lecoq, C. Pézerat, J.-H. Thomas, W.P. Bi, Extraction of the acoustic component of turbulent flow exciting a plate by inverting the vibration problem. *J. Sound Vib.* **333**(2), 2505–92519 (2014)
21. Y. Na, P. Moin, Direct numerical simulation of a separated turbulent boundary layer. *J. Fluid Mech.* **374**, 379–405 (1998)
22. L.J. Peltier, S.A. Hambric, Estimating turbulent boundary layer wall pressure spectra from CFD RANS solutions. *J. Fluids Struct.* **23**, 920–937 (2007)
23. G. Robert, Experimental data base for the pressure gradient effect, EU Contract ENABLE, G4RD-CT-2000-00223 (2002)
24. Y. Rozenberg, G. Robert, S. Moreau, Wall pressure spectral model including the adverse pressure gradient effects. *AIAA J.* **50**(10), 2168–2179 (2012)
25. E. Salze, C. Bailly, O. Marsden, E. Jondeau, D. Juvé, An experimental characterization of wall pressure wavevector-frequency spectra in the presence of pressure gradients. In: 20th AIAA/CEAS Aeroacoustics Conference, AIAA Paper 2014–2909 (2014)
26. H.H. Schloemer, Effects of pressure gradients on turbulent boundary layer wall pressure fluctuations. *J. Acoust. Soc. Am.* **43**(1), 93–113 (1967)
27. A.J. Smits, B.J. McKeon, I. Marusic, High-Reynolds number wall turbulence. *Annu. Rev. Fluid Mech.* **43**, 353–375 (2011)
28. C.K. Tam, L. Auriault, Jet mixing noise from fine scale turbulence. *AIAA J.* **37**(2), 145–153 (1999)

Flinovia - Flow Induced Noise and Vibration Issues and
Aspects

A Focus on Measurement, Modeling, Simulation and
Reproduction of the Flow Excitation and Flow Induced
Response

Ciappi, E.; De Rosa, S.; Franco, F.; Guyader, J.-L.;
Hambric, S.A. (Eds.)

2015, XVII, 358 p. 228 illus., 173 illus. in color.,
Hardcover

ISBN: 978-3-319-09712-1